Hydrogen Interaction with Defects in Nanocrystalline, Polycrystalline and Epitaxial Pd Films

Jakub Čížek[1,a,*], Oksana Melikhova[1,b], Marián Vlček[1,c], František Lukáč[1,d],
Martin Vlach[1,e], Patrik Dobroň[1,f], Ivan Procházka[1,g], Wolfgang Anwand[2,h],
Gerhard Brauer[2,i], Stefan Wagner[3,j], Helmut Uchida[3,k], Ryota Gemma[3,l]
and Astrid Pundt[3,m]

[1]Faculty of Mathematics and Physics, Charles University in Prague,
V Holešovičkách 2, CZ-180 00, Praha 8, Czech Republic

[2]Institut für Strahlenphysik, Helmholtz-Zentrum Dresden Rossendorf,
Postfach 510119, D-01314 Dresden, Germany

[3]Institut fur Materialphysik, Universität Göttingen,
Friedrich-Hund-Platz 1, D-37077 Göttingen, Germany

[a]jakub.cizek@mff.cuni.cz, [b]oksivmel@yahoo.com, [c]marian.vlcek@gmail.com,
[d]frantisek.lukac@gmail.com, [e]martin.vlach@mff.cuni.cz, [f]dobronp@karlov.mff.cuni.cz,
[g]ivan.prochazka@mff.cuni.cz, [h]w.anwand@hzdr.de, [i]g.brauer@hzdr.de, [j]swagner@ump.gwdg.de,
[k]huchida@ump.gwdg.de, [l]Ryota.Gemma@kaust.edu.sa, [m]apundt@ump.gwdg.de

* corresponding author [date of receipt: 7.5.2013 and acceptance: 9.9.2013]

Abstract. Hydrogen interaction with defects and structural development of Pd films with various microstructures were investigated. Nanocrystalline, polycrystalline and epitaxial Pd films were prepared and electrochemically loaded with hydrogen. Structural changes of Pd films caused by absorbed hydrogen were studied by in-situ X-ray diffraction combined with acoustic emission and measurement of electromotorical force. Development of defects during hydrogen loading was investigated by positron annihilation spectroscopy. It was found that hydrogen firstly fills open volume defects existing already in the films and subsequently it occupies also interstitial sites in Pd lattice. Absorbed hydrogen causes volume expansion, which is strongly anisotropic in thin films. This introduces high stress into the films loaded with hydrogen. Acoustic emission measurements revealed that when hydrogen-induced stress achieves a certain critical level rearrangement of misfit dislocations takes place. The stress which grows with increasing hydrogen concentration can be further released by plastic deformation and also by detachment of the film from the substrate.

Introduction

Palladium (Pd) is widely used as a model system for investigations of hydrogen in metal lattice since Pd can absorb a relatively large amount of hydrogen and it can be easily charged with hydrogen [1]. Moreover, Pd is used in hydrogen sensors [2] and hydrogen diffusion membranes [3]. Hydrogen occupies octahedral interstitial sites in fcc Pd lattice and causes remarkable volume expansion [1]. It is known that hydrogen can be trapped at open volume defects like vacancies [4], dislocations [5,6] and grain boundaries [7,8]. This can be explained by positive binding energy of hydrogen to defect, i.e. hydrogen attached to defect exhibits lower energy than hydrogen located at octahedral interstitial site [9]. This explains hydrogen trapping at defects existing already in the material. However, it is known that hydrogen can also introduce new defects into the sample [10]. For example Fukai and Ōkuma [10] discovered extraordinary high vacancy concentration in Pd annealed at high hydrogen pressure of 5 GPa and high temperature of 800°C. Concentration of these hydrogen-induced vacancies is extremely high [11] well above that concentration expected for a metal heated close to its melting temperature. Similarly it has been reported that hydrogen loading introduces dislocations into Pd [12]. Kirchheim [13] showed that hydrogen interaction with defects

can be explained by a decrease of defect formation energy by hydrogen segregating at defect. A new term "defactants = DEFect ACTing AgeNTS" [14] was introduced for solutes segregating at defects and lowering the defect formation energy in analogy to surfactants which reduce surface energies in liquids. Hence, absorbed hydrogen may significantly enhance defect concentration in Pd.

Bulk sample loaded with hydrogen expands in all directions and the lattice expansion increases with increasing hydrogen concentration. On the other hand, a thin film is usually deposited on a stiff substrate which hinders the in-plane expansion. Hence, expansion of a thin film loaded with hydrogen is strongly anisotropic: the in-plane expansion is suppressed, while the out-of-plane expansion is larger than in a free standing sample. This introduces compressive bi-axial in-plane stresses into thin films loaded with hydrogen. These stresses grow with increasing hydrogen concentration and may reach several GPa [15]. Thus, in addition to microstructure hydrogen behavior in thin films, it is influenced also by hydrogen-induced stresses.

In this work we studied hydrogen interaction with defects in thin Pd films. An advantage of thin films is that specimens with various microstructures ranging from single crystalline epitaxial films to nanocrystalline films can be prepared relatively easily by variation of the parameters of deposition procedure. Variable energy slow positron implantation spectroscopy (VEPAS) [16] was employed for characterization of defects in Pd films. VEPAS is a non-destructive technique which provides depth sensitive information about open-volume defects, e.g. vacancies, dislocations, open volumes at grain boundaries etc. VEPAS was combined with structural investigations by synchrotron radiation X-ray diffraction (XRD). Acoustic emission (AE) [17] was employed for *in-situ* investigations of stress release phenomena in the films loaded with hydrogen.

Experimental Details

Samples. Thin Pd films were deposited on polished (11-20) sapphire substrates by cathode beam sputtering in a UHV chamber (10^{-10} mbar) using a Pd target with purity of 99.95%. Three kinds of samples have been prepared: (i) nanocrystalline films deposited at room temperature; (ii) polycrystalline films deposited at room temperature and then annealed in the UHV chamber at a temperature of 800°C for 1 h to initiate grain growth; (iii) epitaxial films deposited at a temperature of 800°C. The thickness of the deposited films was determined by stylus profilometry. Nanocrystalline and polycrystalline films have a thickness of (1080 ± 10) nm and (1040 ± 10) nm, respectively, while epitaxial films have a lower thickness of (485 ± 5) nm.

Techniques. Hydrogen loading was performed by electrochemical cathodic charging in a galvanic cell filled with electrolyte consisting of a mixture of H_3PO_4 and glycerine in the ratio 1:2. The charging was performed step-by-step by constant current pulses between a Pt counter electrode (anode) and the loaded sample (cathode). The current density on the sample was kept at 0.1 mA/cm^2. The hydrogen concentration x_H introduced into the sample can be calculated from the transported charge using the

$$x_H = \frac{ItV_m}{FV},$$

`   (1)

where I is the loading current, t is the duration of the loading pulse, V_m is the Pd molar volume, V is the volume of the loaded film and F is the Faraday's constant. The hydrogen concentration x_H is expressed as atomic ratio H/Pd in the whole paper.

The electromotorical force (EMF) [6], i.e. the electrical potential between the charged sample and a reference Ag/AgCl$_{sat.}$ electrode, was measured to monitor chemical potential of hydrogen absorbed in the films studied. The EMF measurements were carried out with an impedance converter of high input resistance and a digital voltmeter connected to a computer.

VEPAS studies were performed on a magnetically guided positron beam SPONSOR [18] with positron energy adjustable from 0.03 to 36 keV. Doppler broadening of the annihilation line was evaluated using the S (sharpness) line shape parameter [16] calculated as ratio of a suitably selected central area of the annihilation peak (centered at 511 keV) to the net peak area. Usually the central

region is selected so that the S parameter value of a defect-free reference is close to 0.5. In the present work the energy interval was (510.54, 511.46) keV. This choice leads to the value $S_0 = 0.4968(7)$ for a well annealed reference bulk Pd sample at a positron energy $E = 36$ keV. All S parameters reported in this work are normalized to the S_0 value. Localization of a positron in an open-volume defect causes a reduction of positron annihilations with high momentum core electrons and leads to an increase of the S parameter. Thus, S parameter is a measure of the density of open volume defects in the specimen, in case that type of defects remains unchanged.

XRD studies of Pd films were carried out using synchrotron radiation with wavelength of $\lambda = 0.499$ Å in HASYLAB (DESY, Beamline B2) at a beam line equipped with a four-axis Eulerian cradle. The XRD measurements were performed in the Bragg-Brentano symmetrical geometry and the XRD profiles were fitted by the Pearson VII function. The out-of-plane lattice parameters of Pd films were determined from the positions of (111) and (222) Pd reflections using the Cohen Wagner extrapolation plot.

AE was employed for investigations of stress release phenomena in the films loaded with hydrogen. The AE studies were performed *in-situ* during the hydrogen loading using a computer-controlled DAKEL-XEDO-3 AE system. The threshold voltage for the AE count was 480 mV (full scale was ± 2.4 V). A piezoelectric sensor MST8S (a frequency band from 100 to 600 kHz) was attached to the back side on the substrate of the loaded film, while the front side with the Pd film was immersed in the electrolyte.

The morphology of Pd films was examined by scanning electron microscopy (SEM) using a scanning electron microscope JEOL JSM-7500F. Transmission electron microscopy (TEM) was carried out using a Philips CM300SuperTWIN microscope operating at 300 kV. A metallographic light microscope Arsenal AM-2T was used for observations of buckling in the films loaded with hydrogen.

Results and Discussion

Virgin films. TEM micrograph (in cross-section) and SEM image (top view) of the Pd film deposited at room temperature are shown in Figs. 1a and 2a, respectively. The film consists of elongated columns with mean width of ≈50 nm. Fig. 1b shows a high resolution image of one column. XRD profile of the (111) reflection measured in the nanocrystalline film is plotted in Fig. 3a. The reflection has asymmetrical shape indicating that it is actually a superposition of two contributions with slightly different lattice constants. Indeed, on TEM image in Fig. 1a one can distinguish the 'first generation grains' growing directly from the sapphire substrate and the 'second generation grains' growing on the top of the first generation. The dashed line in Fig. 3a shows the position of the (111) reflection in bulk Pd. The (111) reflection for the nanocrystalline Pd films is located at lower diffraction angle than that in bulk Pd. It indicates that the virgin film suffers from in-plane compressive stress imposed by the lattice mismatch with the sapphire substrate, i.e. the film is squeezed in the in-plane directions while in the out-of-plane direction it is expanded. The out-of-plane lattice constants $a_1 = 3.915(4)$ Å and $a_2 = 3.897(5)$ Å were determined in the virgin nanocrystalline film for the first and the second generation grains, respectively. From the difference between the out-of-plane lattice constant in the film and in bulk Pd [1] and using the Young's modulus for Pd $E = 121$ GPa one can estimate that the compressive stress in the virgin nanocrystalline film is $\sigma_1 \approx -0.97$ GPa and $\sigma_2 \approx -0.40$ GPa for the first and the second generation grains, respectively. The compressive strain is higher in the first generation crystallites which are attached directly on the substrate, while in the second generation the stress is more relaxed.

Fig. 2b shows a SEM micrograph of film deposited at room temperature and subsequently annealed at 800°C. Annealing leads to a significant grain growth and changes the nanocrystalline film into polycrystalline with grain size around 2.5 μm. Moreover one can see in Fig. 3b that the shape of (111) reflection for the polycrystalline film becomes symmetrical. It testifies that first and second generation grains merged together during annealing.

High quality of the epitaxial film deposited at 800°C is testified by a sharp and symmetrical XRD reflection plotted in Fig. 3b. Texture measurements performed in Ref. [19] revealed that the epitaxial film is basically monocrystalline with a single orientation with respect to the substrate.
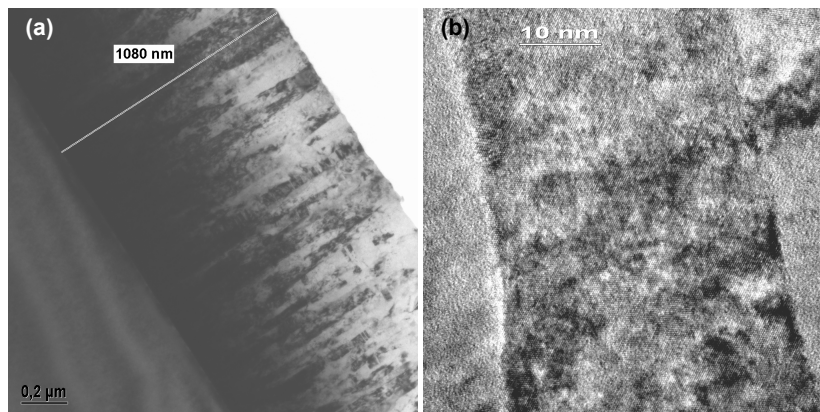

Figure 1 TEM micrographs of the virgin nanocrystalline Pd film: (a) a cross section bright field image, (b) a high resolution image of a column like grain.

The out-of-plane lattice constants a = 3.870(2) Å and 3.876(1) Å were determined for the virgin polycrystalline and epitaxial film, respectively. Hence both these films exhibit a lattice parameter smaller than that of bulk Pd [1]. This indicates that contrary to the nanocrystalline film polycrystalline and epitaxial film exhibit tensile in-plane stress which is caused by lower thermal expansion of sapphire substrate compared to Pd. Hence, shrinkage of the sapphire substrate during cooling of the polycrystalline and the epitaxial film from 800°C is lower than that for the bulk Pd. This induces bi-axial tensile stress with magnitude of 0.42 GPa and 0.26 GPa into the polycrystalline and the epitaxial film, respectively.
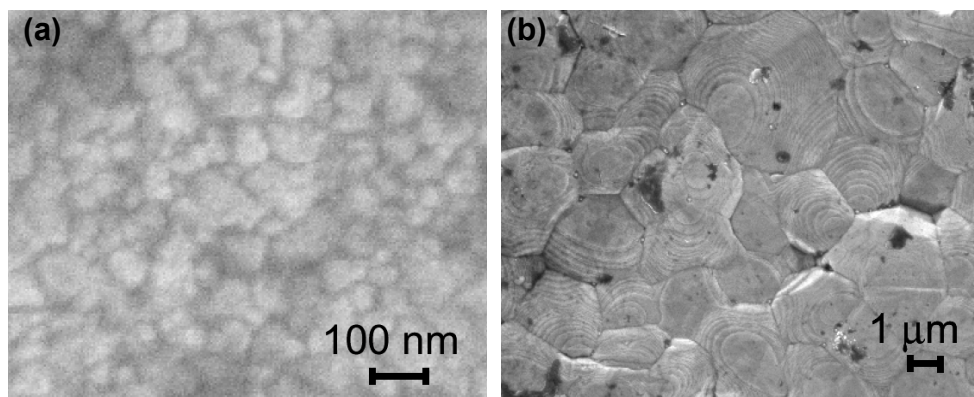

Figure 2 SEM micrographs of virgin Pd films: (a) nanocrystalline film deposited at room temperature, (b) polycrystalline film deposited at room temperature and annealed at 800°C for 1 h.

The dependences of the S parameter on the positron energy E for the virgin films are plotted in Fig. 4a. For comparison the S parameter curve for a well annealed bulk Pd reference sample which can be considered as virtually defect-free material is plotted in the figure as well. At very low energies almost all positrons are annihilated on the surface. With increasing energy positrons penetrate deeper and deeper into the film and the fraction of positrons diffusing back to the surface decreases. This is reflected by a decrease of the S parameter from the surface value to the bulk value corresponding to the situation when all positrons are annihilated inside Pd. From inspection of Fig. 4a it becomes clear that the virgin nanocrystalline film exhibits a bulk S parameter which is remarkably higher than that in the well annealed bulk Pd. It testifies that the nanocrystalline Pd film exhibits relatively high concentration of defects already in the virgin state. This is due to its nanocrystalline structure which leads to a significant volume fraction of grain boundaries containing open volume defects. Hence, in the nanocrystalline film majority of positrons diffuse to grain

boundaries and are trapped at open volume defects there. Annealing of nanocrystalline film at 800°C obviously leads to a recovery of defects reflected by a decrease of the bulk S parameter. But the epitaxial film exhibits very high bulk S parameter which testifies to a high density of defects due to a dense network of misfit dislocations compensating for the lattice mismatch with the substrate. The average dislocation density of 2×10^{16} m^{-2} was estimated for the epitaxial film [19].

Figure 3 Profile of the (111) Pd reflection measured by XRD on virgin Pd films (a) nanocrystalline film deposited at room temperature, (b) polycrystalline film deposited at room temperature and annealed at 800°C for 1h (open squares left y-axis scale) and epitaxial film deposited at 800°C (open circles, right y-axis scale). The solid lines show a fit of the reflections by a Pearson VII model function. In case of the nanocrystalline film (left panel) the model function consists of a contribution of the first and the second generation crystallites shown by dashed lines. The position of the (111) Pd reflection in a perfect Pd crystal is indicated by a vertical dashed line.
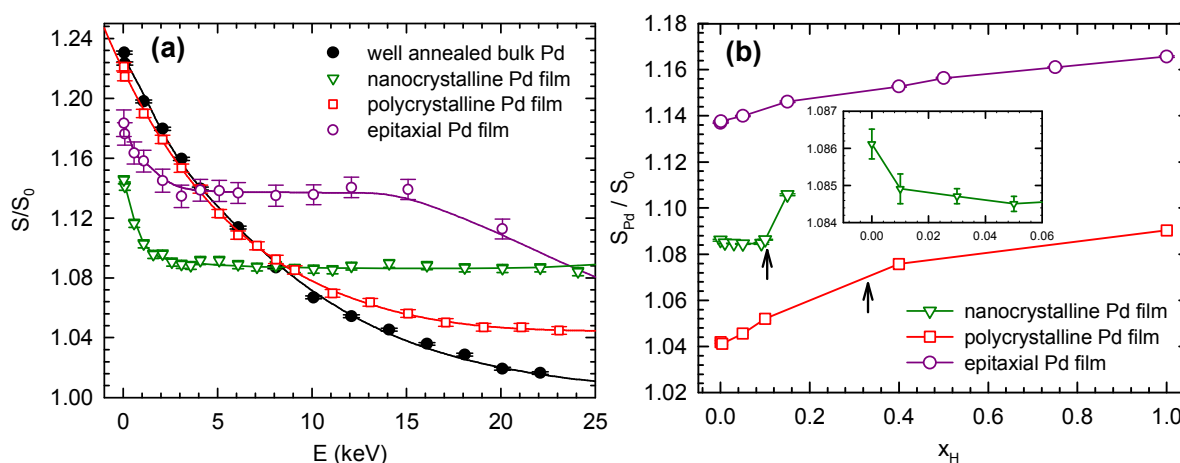

Figure 4 VEPAS results: (a) dependence of the S parameter on positron energy E for virgin films and a reference well annealed bulk Pd sample; (b) bulk S parameter S_{Pd} for Pd layer plotted as a function of hydrogen concentration x_H. Arrows in the figure indicate the onset of buckling in the nanocrystalline and the polycrystalline film. The inset shows a detail of S parameter development in the nanocrystalline film at low hydrogen concentrations.
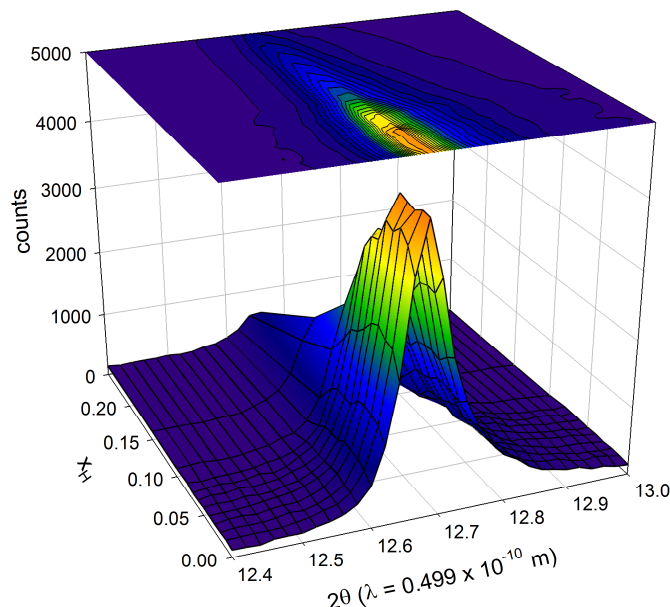
Figure 5 The development of XRD profile for the (111) reflection measured on the nanocrystalline film loaded with hydrogen.
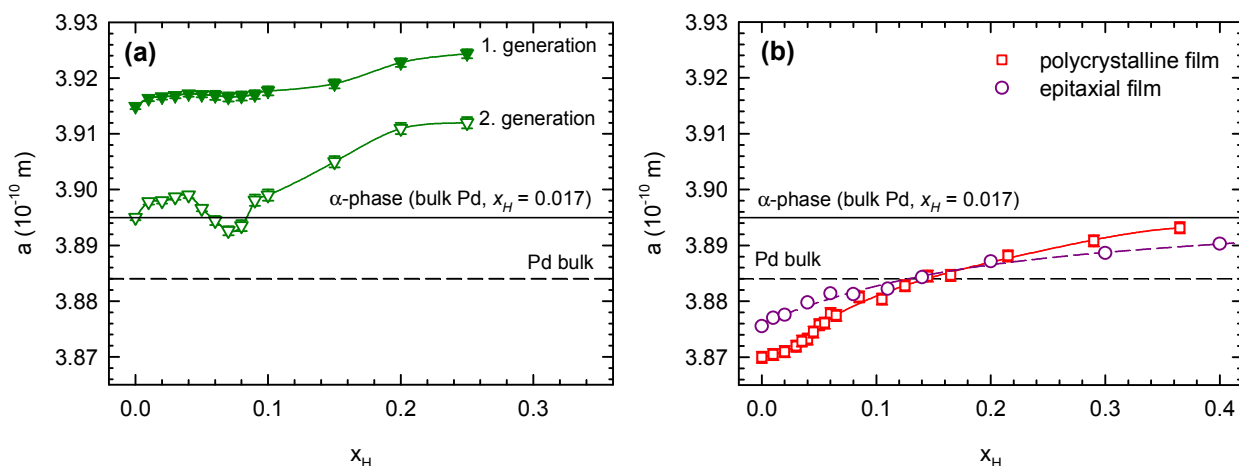

Figure 6 The dependence of the out-of-plane lattice parameters on hydrogen concentration: (a) nanocrystalline film; (b) polycrystalline and epitaxial film. Solid vertical line shows the lattice parameter of bulk pure Pd, dashed line shows the lattice parameter for α-phase in bulk Pd containing hydrogen concentration $x_H = 0.017$.

Films loaded with hydrogen. Fig. 5 shows the behavior of the (111) Pd reflection measured on the nanocrystalline film loaded with hydrogen. The asymmetrical shape of the reflection remains during hydrogen loading testifying that the difference in the lattice constant between the first and the second generation crystallites remains. The (111) reflection firstly shifts to lower diffraction angles due to out-of-plane lattice expansion caused by absorbed hydrogen. During further loading the reflection becomes broader and its intensity decreases which indicates plastic deformation of the film. When hydrogen concentration approaches $x_H \approx 0.1$ hydrogen-induced stresses exceed the film adhesion to the substrate and buckles are formed in the film [20,21]. Film detachment from the substrate starts on edges but during further loading buckling takes place in the whole film. One can see in Fig. 5 that buckling leads to a drastic drop of intensity of the (111) reflection due to misalignment of the film. No formation of α' phase was observed up to hydrogen concentration $x_H \approx 0.25$ where the loading was stopped because the film was almost completely detached from the substrate. The out-of-plane lattice constant for the first and the second generation grains determined from fitting of XRD data is plotted in Fig. 6a as a function of hydrogen concentration in the film. The lattice constant firstly increases due to lattice expansion. However, at hydrogen concentration

$x_H \approx 0.04$ in-plane relaxation occurs and the lattice constant of the second generation crystallites returns approximately to the value corresponding to the lattice parameter of the α phase in bulk Pd [1]. Some in-plane stress relaxation although smaller in magnitude can be seen also in the first generation crystallites which suffer from significantly higher in-plane stress. During further loading the out-of-plane lattice parameter increases again. At hydrogen concentration $x_H \approx 0.10$ buckling of the film begins. Detached parts of the film are not fixed at the substrate anymore and can expand in all directions.
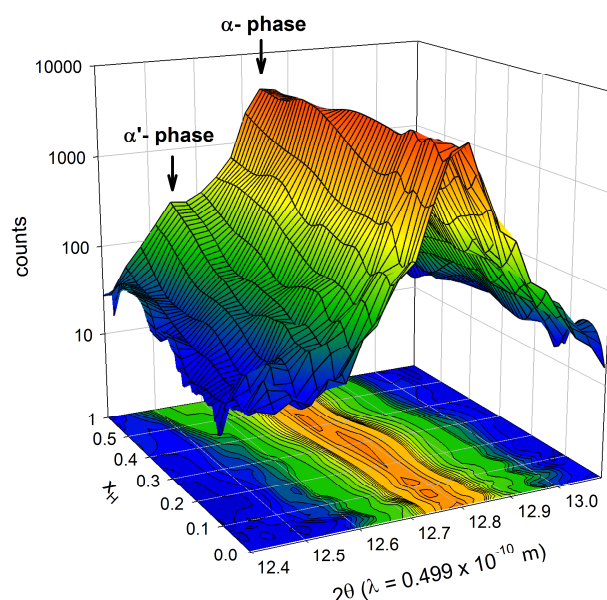

Figure 7 The development of XRD profile of the (111) reflection for the polycrystalline film loaded with hydrogen. The peaks corresponding to α and α' phase are indicated by arrows.

XRD data for the polycrystalline and the epitaxial Pd film loaded with hydrogen are shown in Figs. 7 and 8, respectively. In both films the (111) reflection is firstly shifted to lower diffraction angles due to hydrogen-induced out-of-plane expansion. Subsequently phase transition from α-phase to α'-phase takes place. This behavior is comparable with bulk Pd, but both polycrystalline and epitaxial exhibit higher hydrogen solubility in the α-phase than bulk Pd. In the polycrystalline film buckles are formed at $x_H > 0.3$, while in the epitaxial film no buckles were observed during the whole loading procedure, i.e. up to $x_H \approx 1$. This testifies that by film deposition at elevated temperature good bonding between the Pd film and sapphire substrate has established. The out-of-plane lattice parameters for α-phase determined in the polycrystalline and the epitaxial film are plotted in Fig. 6b as a function of hydrogen concentration. In both films the lattice parameter monotonically increases and approaches the value for α-phase in bulk Pd. Hence, contrary to the nanocrystalline film in-plane relaxation was not detected in the polycrystalline and the epitaxial film most probably because these films exhibit tensile in-plane stress in the virgin state.

Fig. 4b shows the dependence of the bulk S parameter on the hydrogen concentration for the Pd films studied. The whole $S(E)$ curves measured at various hydrogen concentrations can be found in Ref. [19]. From inspection of Fig. 4b one can conclude that in the polycrystalline and the epitaxial film the S parameter monotonically increases with increasing hydrogen concentration testifying to formation of new defects during hydrogen loading. It indicates that in polycrystalline and epitaxial film hydrogen-induced stress is released by plastic deformation which introduces dislocations. On the other hand, in the nanocrystalline film S parameter firstly decreases, see the inset in Fig. 4b, because hydrogen fills open volume defects at grain boundaries. At hydrogen concentrations $x_H >$ 0.02 all available deep traps at grain boundaries are already filled and S remains approximately constant. When hydrogen concentration exceeds $x_H \approx 0.1$ buckling takes place leading to a strong increase of S parameter and testifying that plastic deformation takes place during buckling.

Left panels in Fig. 9 show cumulative number of AE counts detected in the films during hydrogen loading. In the nanocrystalline film there is a region at low hydrogen concentrations where no AE counts have been detected. Subsequently a few isolated AE events appeared, see Fig. 9a. These AE events are most probably related to stress release by the in-plane relaxation which was detected also by XRD. Since VEPAS data did not show any increase of defect concentration in this range of hydrogen concentrations the stress release is likely caused by rearrangement of misfit dislocations existing already in the film. Buckling of the film which takes place at $x_H > 0.1$ leads to a huge increase in the number of AE counts. This testifies that severe plastic deformation takes place during buckling leading to a collective movement of many dislocations which is in accordance with VEPAS results.
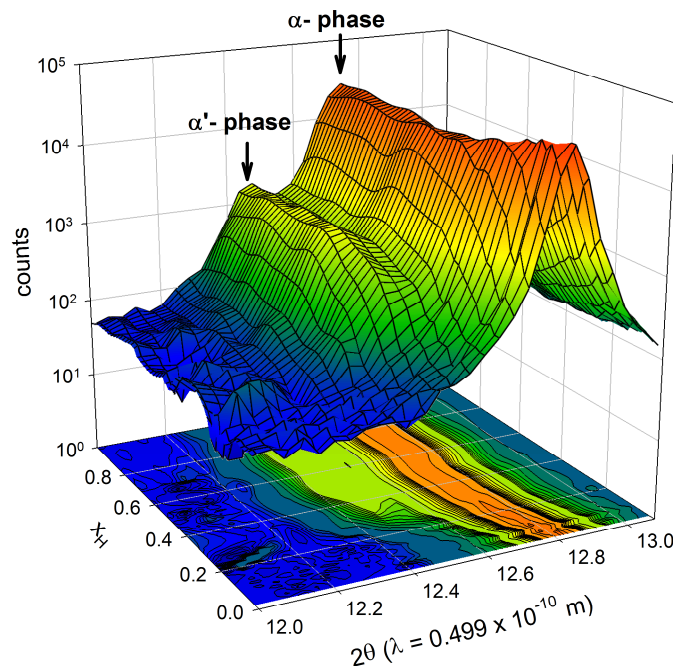

Figure 8 The development of XRD profile of the (111) reflection measured in the epitaxial film loaded with hydrogen. The peaks corresponding to α and α' phase are indicated by arrows.

In the polycrystalline film (Fig. 9c) there is also a region at low x_H where no AE signals could be detected. First isolated AE events were detected at $x_H \approx 0.06$. Similarly to the nanocrystalline film these AE events are most probably caused by stress release due to rearrangement of misfit dislocations. However, because of tensile in-plane stress in the virgin polycrystalline film the stress induced by absorbed hydrogen is lower and stress relaxation takes place at higher hydrogen concentration than in the nanocrystalline film. Plastic deformation takes place during further loading and leads to a strong increase in the number of AE counts. Finally at $x_H > 0.3$ buckling occurs and further enhances the number of AE events. In contrast to this, in the epitaxial film AE signals were observed already from the beginning of hydrogen charging and appeared continuously during the whole loading procedure. It indicates that in the epitaxial film plastic deformation takes place during whole loading and continuously dislocations are created in the film.

Right panels in Fig. 9 show the dependence of equilibrium EMF on hydrogen concentration for the nanocrystalline, the polycrystalline and the epitaxial film. The Sivert's law predicts that solubility of hydrogen expressed by concentration of hydrogen x_H absorbed in a sample is proportional to the square root of hydrogen partial pressure p_{H_2}

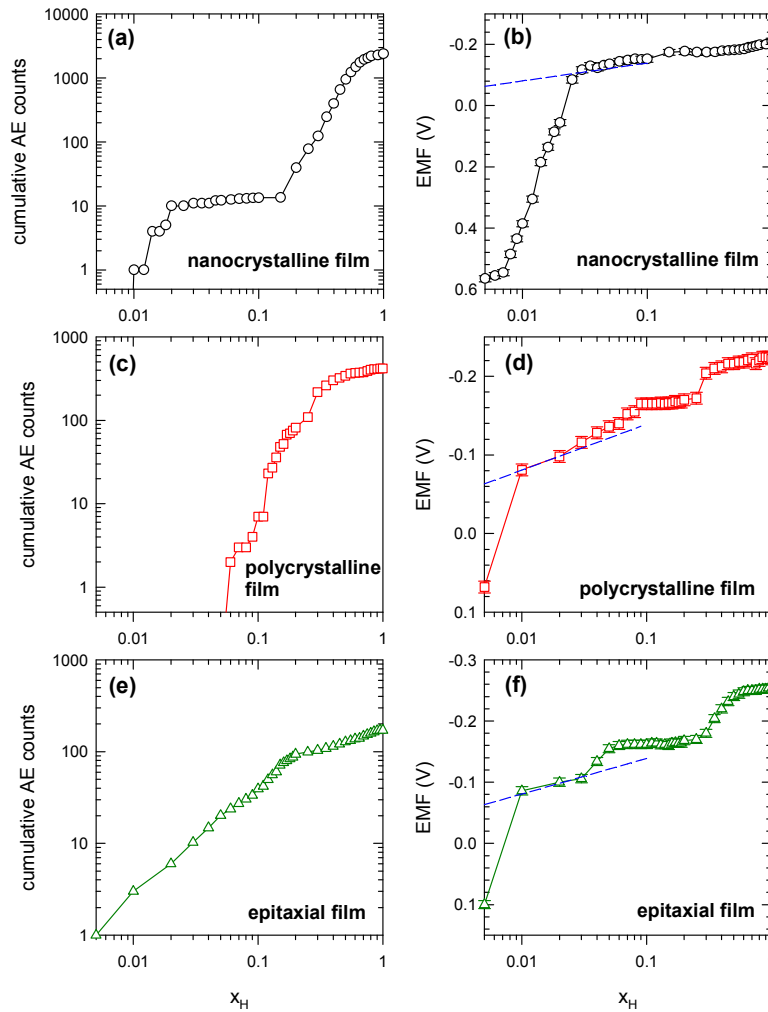$$x_H = \exp\left(\frac{\Delta G^0}{RT}\right)\sqrt{p_{H_2}} , \qquad (2)$$

Figure 9 Cumulative number of AE counts and equilibrium EMF for hydrogen loaded Pd films.

where R is the gas constant, T is thermodynamic temperature and the change of Gibbs free energy ΔG^0 is directly related to the standard EMF [6]

$$\Delta G^0 = \left(EMF - E_{ref} \right) F. \qquad (3)$$

In the latter equation F is the Faraday's constant and the reference potential E_{ref} = -0.197 V for the Ag/AgCl$_{sat}$ electrode. Combining Eqs. (2) and (3) and assuming standard condition p_{H_2} = 1 bar the Sievert's law or ideal solution behavior can be formulated as a linear relation between EMF and the logarithm of the concentration of absorbed hydrogen

$$EMF = E_{ref} - \frac{RT}{F} \ln x_H. \qquad (4)$$

The linear relation given expressed by Eq. (4) is shown in the right panels of Fig. 9 by a dashed line. One can see in Fig. 9 that in all films studied there is always certain region where hydrogen fills interstitial sites in Pd lattice and the Sivert's law is fulfilled. However, a strong deviation from the Sievert's behavior was observed at low hydrogen concentrations because hydrogen preferentially fills open volume defects in the film. The hydrogen trapping region is most extended in the nanocrystalline film where hydrogen is trapped at grain boundaries. At high x_H buckling takes place and in the polycrystalline and the epitaxial film also phase transition to α' phase. Both these processes cause deviations from the Sievert's law behavior.

Summary

In summary hydrogen interaction with defects was studied in nanocrystalline, polycrystalline and epitaxial Pd films. Absorbed hydrogen firstly fills open-volume defects existing in the films. Subsequently, hydrogen-induced stress is released by rearrangement of misfit dislocations. During further hydrogen loading the stress induced by absorbed hydrogen can be released by plastic deformation and buckling of the film. The latter two processes are likely promoted by hydrogen acting as defactant, segregating at dislocations and free surfaces and, thereby, lowering the formation energies of these defects.

Acknowledgement

References

[1] T.B. Flanagan, W.A. Oates, The palladium-hydrogen system, Annu. Rev. Mater. Sci. 21 (1991) 269-304.

[2] P. Kumar, L. Malhotra, Palladium capped samarium thin films as potential hydrogen sensors, Mater. Chem. Phys. 88 (2004) 106-109.

[3] A. G. Knapton, Palladium Alloys for Hydrogen Diffusion Membranes, Platinum Metals Rev. 21 (1977) 44-50.

[4] A. Pundt, R. Kirchheim, Hydrogen in metals: microstructural aspects, Annu. Rev. Mater. Res. 36 (2006) 555-608.

[5] R. Kirchheim, Hydrogen solubility and diffusivity in defective and amorphous metals, Prog. Mater. Sci. 32 (1988) 261-325.

[6] R. Kirchheim, Interaction of hydrogen with dislocations in palladium—I. Activity and diffusivity and their phenomenological interpretation, Acta Metall. 29 (1981) 835-843.

[7] T. Mütschele, R. Kirchheim, Segregation and diffusion of hydrogen in grain boundaries of palladium, Scripta Metall. 21 (1987) 135-140.

[8] T. Mütschele, R. Kirchheim, Hydrogen as a probe for the average thickness of a grain boundary, Scripta Metall. 21 (1987) 1101-1104.

[9] F. Besenbacher, J.K. Norskow, M.J. Puska, S. Holloway, Interaction of hydrogen with defects in metals, Nucl. Instrum. Methods Phys. Res. B 7-8 (1985) 55-66.

[10] Y. Fukai, N. Ōkuma, Evidence of Copious Vacancy Formation in Ni and Pd under a High Hydrogen Pressure, Jpn. J. Appl. Phys. 32 (1993) L1256-L1259.

[11] Y. Fukai, N. Ōkuma, Formation of Superabundant Vacancies in Pd Hydride under High Hydrogen Pressures, Phys. Rev. Lett. 73 (1994) 1640-1643.

[12] R.D. Field, D.J. Thoma, In-situ hydrogen charging of Pd and Pd-Rh in the TEM, Scripta Mater. 37 (1997) 347-353.

[13] R. Kirchheim, Reducing grain boundary, dislocation line and vacancy formation energies by solute segregation. I. Theoretical background, Acta Mater. 55 (2007) 5129-5138.

[14] R. Kirchheim, On the solute-defect interaction in the framework of a defactant concept, Int. J. Mater. Res. 100 (2009) 483-487.

[15] A. Pundt, M. Getzlaff, M. Bode, R. Kirchheim, R. Wiesendanger, H-induced plastic deformation of Gd thin films studied by STM, Phys. Rev. B 61 (2000) 9964-9967.

[16] P.J. Schultz, K.G. Lynn, Interaction of positron beams with surfaces, thin films, and interfaces, Rev. Mod. Phys. 60 (1988) 701-779.

[17] M.A. Hamstad, A Review: Acoustic Emission as a Tool for Composite Materials Studies, Experimental Mechanics 26 (1986) 7-13.

[18] W. Anwand, G. Brauer, M. Butterling, H.-R. Kissenger, A. Wagner, Design and Construction of a Slow Positron Beam for Solid and Surface Investigations, Defect and Diffusion Forum 331 (2012) 25-40.

[19] J. Čížek, O. Melikhova, M. Vlček, F. Lukáč, M. Vlach, I. Procházka, W. Anwand, G. Brauer, A. Mücklich, S. Wagner, H. Uchida, A. Pundt, Hydrogen-induced microstructural changes of Pd films, Int. J. Hydrogen Energy 38 (2013), 12115-12152.

[20] A. Pundt, P. Pekarski, Buckling of thin niobium-films on polycarbonate substrates upon hydrogen loading, Scripta Mater. 48 (2003) 419-423.

[21] A. Pundt, E. Nikitin, P. Pekarski, R. Kirchheim, Adhesion energy between metal films and polymers obtained by studying buckling induced by hydrogen, Acta Mater. 52 (2004)1579-1587.

Hydrogen Interaction with Defects in Nanocrystalline, Polycrystalline and Epitaxial Pd Films